A High-frequency Geodetic VLBI Experiment for Optical Clock Comparison

Original
A High-frequency Geodetic VLBI Experiment for Optical Clock Comparison / Negusini, Monia; Heo, Myoung-Sun; Clivati, Cecilia; Xu, Shuangjing; Ricci, Roberto; Jung, Taehyun; Cho, Buseung; Stagni, Matteo; Bortolotti, Claudio; Maccaferri, Giuseppe; Perini, Federico; Roma, Mauro; Byun, Do-Young; Je, Do-Heung; Pizzocaro, Marco; Calonico, Davide; Cantoni, Elena; Cerretto, Giancarlo; Condio, Stefano; Costanzo, Giovanni A.; Donadello, Simone; Goti, Irene; Gozzelino, Michele; Mura, Alberto; Levi, Filippo; Risaro, Matias; Kim, Huidong; Lee, Won-Kyu; Park, Chang Yong; Yu, Dai-Hyuk; Lee, Young Kyu; Rhee, Joon Hyo; Park, Chanjin; Lee, Minseong; Kim, Hyo Ryoung; Yoo, Sung-Moon; Choi, Jungho; Kim, Jongsoo; Yi, Sang-Oh; Yoon, Ha Su; De Vicente, Pablo; González, Javier; García Miró, Cristina. - In: PUBLICATIONS OF THE ASTRONOMICAL SOCIETY OF THE PACIFIC. - ISSN 0004-6280. - 138:2(2026). [10.1088/1538-3873/ae36d1]

Availability:
This version is available at: 11696/88361 since: 2026-02-26T21:55:22Z

Publisher:
IOP Publishing Ltd

Published
DOI:10.1088/1538-3873/ae36d1

Publications of the Astronomical Society of the Pacific, 138:024504 (10pp), 2026 February https://doi.org/10.1088/1538-3873/ae36d1

A High-frequency Geodetic VLBI Experiment for Optical Clock Comparison

Monia Negusini[1], Myoung-Sun Heo[2], Cecilia Clivati[3], Shuangjing Xu[4], Roberto Ricci[1,5], Taehyun Jung[4], Buseung Cho[6], Matteo Stagni[1], Claudio Bortolotti[1], Giuseppe Maccaferri[1], Federico Perini[1], Mauro Roma[1], Do-Young Byun[4,7], Do-Heung Je[4], Marco Pizzocaro[3], Davide Calonico[3], Elena Cantoni[3], Giancarlo Cerretto[3], Stefano Condio[3], Giovanni A. Costanzo[3,8], Simone Donadello[3], Irene Goti[3], Michele Gozzelino[3], Alberto Mura[3], Filippo Levi[3], Matias Risaro[3], Huidong Kim[2], Won-Kyu Lee[2], Chang Yong Park[2], Dai-Hyuk Yu[2], Young Kyu Lee[2], Joon Hyo Rhee[2], Chanjin Park[6], Minseong Lee[6], Hyo Ryoung Kim[4], Sung-Moon Yoo[4], Jungho Cho[4], Jongsoo Kim[4,7], Sang-Oh Yi[9], Ha Su Yoon[9], Pablo de Vicente[10], Javier González[10], and Cristina García Miró[10]

[1] Institute for Radio Astronomy, National Institute for Astrophysics, Via Piero Gobetti 101, Bologna, 40129, Italy; monia.negusini@inaf.it, c.bortolotti@ira.inaf.it, m.roma@ira.inaf.it

[2] Korea Research Institute of Standards and Science, 267 Gajeong-ro, Yuseong-gu, Daejeon, 34113, Republic of Korea

[3] Quantum Metrology and Nanotechnology division, Istituto Nazionale di Ricerca Metrologica, Strada delle cacce 91, Torino, 10135, Italy; matias.risaro@npl.co.uk

[4] Korea Astronomy and Space Science Institute, 776 Daedeok-daero, Yuseong-gu, Daejeon, 34055, Republic of Korea

[5] Dipartimento di Fisica, Università di Roma Tor Vergata, Via della ricerca scientifica 1, Roma, 00133, Italy

[6] Korea Institute of Science and Technology Information, 245 Daehak-ro, Yuseong-gu, Daejeon, 34141, Republic of Korea

[7] University of Science and Technology, Gajeong-ro 217, Yuseong-gu, Daejeon, 34113, Republic of Korea

[8] Electronics and Telecommunications Department, Politecnico di Torino, Corso Duca degli Abruzzi 124, Torino, 10134, Italy

[9] National Geographic Information Institute, 92 Worldcup-ro, Yeongtong-gu, Suwon-si, 443-772, Republic of Korea

[10] Yebes Observatory, Instituto Geográfico Nacional, Cerro de la Palera, Yebes, Guadalajara, 19143, Spain

Received 2025 July 16; revised 2026 January 8; accepted 2026 January 12; published 2026 February 10

Abstract

An intercontinental metrological clock comparison between Italy and the Republic of Korea was performed by means of geodetic *K*-band VLBI observations. The comparison involved the hydrogen masers (H-masers) used at Medicina and Sejong radio telescopes. The same clocks were simultaneously compared by a satellite link and by high-precision optical clocks maintained at the National Metrology Institutes, KRISS in Korea and INRIM in Italy, and delivered to VLBI antennas via optical fiber. The H-masers frequency difference was estimated by extrapolating the clock rate from VLBI data using two geodetic VLBI software. This was subsequently compared with clock differences derived by satellite link and by local optical clocks. Results obtained with different approaches were in agreement at the level of $10^{-15}\,\mathrm{s\,s^{-1}}$. This pilot study demonstrates that standard high-frequency (*K*-band) geodetic VLBI campaigns could be a viable approach to conduct intercontinental clock comparisons, now only possible via satellite links. This uncertainty can be reduced thanks to the planned installation of new-generation, broadband, high-frequency receivers on the involved telescopes. $K/Q/W$-band geodetic observations will allow an improvement of the accuracy of the resulting group delays through broad bandwidth synthesis from 20 to 100 GHz. Furthermore, the Frequency Phase Transfer method will also be explored together with the use of PCAL systems installed at the radio telescopes to improve phase stability and thus allow a better estimation of the station clock parameters.

Unified Astronomy Thesaurus concepts: Very long baseline interferometry (1769); Astronomical instrumentation (799); Astronomical methods (1043); Quasars (1319)

1. Introduction

Very Long Baseline Interferometry (VLBI) is one of the scientific fields that most heavily relies on accurate time and frequency reference signals, demonstrating significant synergy with fundamental metrology. It is based on the simultaneous observations of radio sources with an array of telescopes, each referenced to a local frequency standard. By correlating the radio signals received by the various telescopes it is possible to reconstruct pair-wise propagation delays, that depend on the baseline length and orientation, atmospheric effects and ultimately the radio source position and structure (Schuh & Behrend 2012). Discrepancies in the local clock frequencies and instrumental delays may also play a role. When all effects are taken into account, it is possible for VLBI to reconstruct with good fidelity rich information, e.g., on the position of the

radio telescopes, the Earth Orientation Parameters (EOPs), the source positions and structure. Specifically, VLBI and frequency metrology can take mutual advantage from each other: on one side, VLBI resolution could be greatly improved with instrumentation and techniques that are traditionally maintained at Metrological Institutes. These include atomic clocks with state-of-the-art accuracy, today at the 10^{-18} level (Ushijima et al. 2015; McGrew et al. 2018; Brewer et al. 2019; Beloy et al. 2021), useful to investigate phenomena over timescales of months or years (Krishnan et al. 2020); high spectral purity oscillators (Xie et al. 2017; Nakamura et al. 2020), crucial in mm- and sub-mm-wavelength observations (Raymond et al. 2024); sub-ns synchronization of remote sites (Serrano et al. 2009; Dierikx et al. 2016) and distribution of atomic clock signals to multiple telescopes via optical fiber, that enable to realize distributed common-clock arrays (Krehlik et al. 2017; Clivati et al. 2020; Boven et al. 2026). On the other side, atomic clocks connected to the telescope can be compared worldwide via VLBI. This is important for fundamental metrology, as discussion is ongoing on a future redefinition of the second in the International System of units (Gill 2016; Riehle et al. 2018; Lodewyck 2019; Dimarcq et al. 2024). Comparing distant atomic clocks is among the most urgent tasks to gain confidence on the best route to redefinition. Moreover, it allows fundamental physics tests at unprecedented resolution (Sanner et al. 2019; Lange et al. 2021), as well as advanced relativistic geodesy measurements (Grotti et al. 2018; McGrew et al. 2018; Takamoto et al. 2020). However, clock comparisons represent a challenging task: while regional distances can be covered with fiber optic links (Musha et al. 2008; Droste et al. 2013; Chiodo et al. 2015; Lisdat et al. 2016; Akatsuka et al. 2020; Clivati et al. 2020; Husmann et al. 2021; Clivati et al. 2022), intercontinental clock comparisons are mostly conducted using the Global Navigation Satellite Systems (GNSS), though their performance may not meet the accuracy required for the redefinition (Bauch et al. 2005; Fujieda et al. 2014; Hachisu et al. 2014; Leute et al. 2016; Riedel et al. 2020; Pizzocaro et al. 2021).

Since the end of the 1970s, the geodetic VLBI has been using the S/X band receivers with the aim of monitoring the parameters of the Earth's orientation, studying the movements of the Earth's crust and other geophysical phenomena, realizing the international terrestrial and celestial reference frames (ITRF and ICRF). Its application for time and frequency transfer has been investigated since the beginning (e.g., Counselman et al. 1977; Clark et al. 1979; Hurd et al. 1979) and an uncertainty of 1.5×10^{-15} for a time period of 1 day has been reported in an earlier study (Rieck et al. 2012). For local H-masers, which have a relative frequency instability well below 10^{-12}, the VLBI-determined clock rate is equivalent to the rate of one clock relative to that of the other clock (Sekido et al. 2021). The uncertainties that can be achieved with legacy S/X band observations are not sufficient for optical clocks comparison, so new possibilities are being explored, such as VLBI observations performed with broadband receivers.

In 2018/19, an intercontinental comparison of optical clocks was carried out using a broadband VLBI link between Italy and Japan with an uncertainty of 2.8×10^{-16}, lower than that achievable by a satellite link and thus particularly promising in a metrological perspective (Pizzocaro et al. 2021). However, in that campaign data were collected and analyzed under very special constraints, such as small transportable antennas and broadband NINJA feeds (3–14 GHz) and a direct digitization without baseband conversion (Sekido et al. 2021). A new generation of a high-frequency broadband receiver (>20 GHz) is beginning to become available globally among VLBI communities, which would be highly effective in calibrating tropospheric phase fluctuations in the millimeter waveband, significantly enhancing the precision of group delay measurements through broad bandwidth synthesis from 20 to 100 GHz. Moreover, they have the potential to reduce frequency-dependent systematic errors, such as source structure ones. The visible source structure on larger scales induces non-closure delays, increasing post-fit delay residuals in geodetic solutions, while the invisible structure within the beam size leads to variations in the source position (Xu & Charlot 2025). Given the influence of in-beam structure on source positions, the transition to higher radio frequencies may be important for astrometry and geodesy. To fully exploit its potential, a highly stable local frequency reference is required as stated in (Rioja & Dodson 2020) and (Ledbetter et al. 2025). Rather than installing a new local reference at each site, accurate clocks delivered via optical fiber links offer a promising alternative. These advantages can be beneficial for accurate clock comparison using VLBI.

A project involving the Korea Astronomy and Space Science Institute (KASI) and the Italian Institute of Astrophysics (INAF) allows the installation of Korean Compact Triple-band Receivers (CTRs) that operate simultaneously in the K (18-26 GHz), Q (35–50 GHz), and W (85–115 GHz) bands (Han et al. 2017) on all three INAF radio telescopes (Medicina, Noto, and SRT). Waiting for the installation and commissioning phases to be completed, we explore the use of an intercontinental network of operational high-frequency VLBI antennas to conduct metrological clock comparisons. Importantly, our strategy was to exploit procedures and instrumentation that are routinely used at most radio telescopes today. This would leverage the use of the existing VLBI network for various scientific tasks, including metrology. Our test campaigns were thus conducted as geodetic ones, with K-band observations and standard scheduling and analysis, with the aim to identify ultimate limits, critical aspects and achievable metrological performances.

This paper will describe the international network, experimental setup and analysis procedures, and discuss current

results and future perspectives. Specifically in Section 2 the basics of geodetic VLBI are presented and the VLBI-clock comparison experiment is explained, in Section 3 the VLBI observations and geodetic data analysis are presented. In Section 4 the comparison via VLBI, optical clocks and GNSS are shown; in Section 5 the results are discussed and some conclusion and outlook are drawn in Section 6.

2. VLBI-clock Comparison Experiment

2.1. VLBI Basics

Geodetic VLBI is based on the simultaneous observation of extragalactic radio sources (usually quasars) with distant antennas. The main observable is the difference in arrival times (time delay) of the radio signal from a radio source to two or more globally distributed radio telescopes. This time delay $\tau_{\rm obs}$, measured to a precision of a few picoseconds using highly stable atomic clocks (hydrogen masers) at each station, is the fundamental measurement used to derive essential geodetic and astrometric parameters, including precise positions and velocities of the telescopes, positions of quasars, and Earth orientation parameters, such as universal Time (UT1), which describes the Earth's rotation angle. Indeed, the geometric delay between two stations, $\tau_{\rm geom} = \boldsymbol{B} \cdot \boldsymbol{S}/c$, depends on the baseline vector between the antennas (**B**) and the unit vector of the radio source (**S**), where c is the speed of light. The observed value $\tau_{\rm obs}$ differs from the geometric delay due to a number of different effects, such as the time offset between the reference clocks $\Delta\tau_{\rm clock}$, the station-to-station difference in the excess delays introduced by the neutral (troposphere, $\Delta\tau_{\rm tro}$) and the ionized (ionosphere, $\Delta\tau_{\rm ion}$) part of the atmosphere, instrumental delays such as antennas, cables and receivers $\Delta\tau_{\rm instr}$ and finally the structure of the radio source $\Delta\tau_{\rm source}$:

$$\tau_{\rm obs} = \tau_{\rm geom} + \Delta\tau_{\rm tro} + \Delta\tau_{\rm ion} + \Delta\tau_{\rm instr} + \Delta\tau_{\rm source} + \Delta\tau_{\rm clock} \quad (1)$$

The different components of the delay can be modeled, estimated from the observations or obtained as a result of external measurements. Typically, geodetic VLBI experiments last 24 hr, involving a network of stations and observing a number of spatially distributed radio sources with very well known positions in order to have a good coverage of the sky and thus be able to estimate with very good accuracy the positions of the radio telescopes, the atmospheric delays and the clock behavior.

2.2. Experiment Setup

In this work, we compare the frequencies of H-masers used in VLBI observations at Medicina and Sejong radio telescopes via a VLBI geodetic link by measuring $\Delta\tau_{\rm clock}$ as described in the previous section and, simultaneously, by calibration to high-precision Yb optical clocks, KRISS-Yb1 and IT-Yb1, maintained at the National Metrology Institutes (NMIs) Korea Research Institute of Standards and Science (KRISS) in Korea and Istituto Nazionale di Ricerca Metrologica (INRIM) in Italy, respectively (Figure 1). During the VLBI sessions, a GNSS link based on GPS Precise Point Positioning (PPP) was operational between INRIM and KRISS for consistency check and comparison.

Throughout this work, the quantity directly compared by VLBI is the fractional frequency difference between the two H-masers; the optical clocks and the GPS link are used to calibrate these masers and to provide an external reference for evaluating the VLBI link itself.

2.3. VLBI Setup

A network of six radio telescopes between Europe and the Republic of Korea was involved in the *K*-band 24 hr geodetic session: Medicina 32 m antenna (Italy, operated by INAF) and Yebes 40 m antenna (Spain, operated by the Yebes Astronomical Centre) in Europe (Figure 1(d)), and Sejong 22 m antenna (operated by the National Geographic Information Institute—NGII) and the three Yonsei, Ulsan and Tamna 21 m Korean VLBI Network antennas (KVN, operated by KASI), in Korea (Figure 1(e)). The Yebes antenna was involved in the experiment to balance the geometry of the network between Europe and Korea and to provide additional observations to improve the overall statistics of the observing session and the estimation of interesting parameters, by increasing the number of baselines. The Sejong station receives a clock signal (10 MHz) from a hydrogen maser at KRISS via the optical fiber of the Korea Research Environment Open Network (KREONET), a national research and science network operated by the Korean Institute of Science & Technology Information (KISTI) (Figure 1(c)). The delivered signal is demodulated and multiplied to 1.4 GHz, to feed into the Round Trip System (RTS) (Oh et al. 2010), which sends the 1.4 GHz signal to the antenna receiver room for VLBI observation with the fiber-induced noise suppressed. At Medicina station, in Italy, the local H-maser is used for VLBI observations, but its frequency is constantly measured against a clock signal delivered from INRIM over the Italian Quantum Backbone (IQB), a fiber infrastructure for metrological time and frequency distribution in the whole country (Figures 1(a) and (b)). More details on the fiber-based clock distribution to the two telescopes are given in Section 2.4. The experiment schedule was generated using NASA's software *SKED* (Gipson 2010), which is widely used to schedule geodetic and astrometric VLBI observations. We compiled a catalog with over 230 sources, which are included in the ICRF3 *K*-band catalog (Charlot et al. 2020) and generally strong (>0.4 Jy at *K* or *X* band), flat-spectrum sources in the Radio Fundamental Catalog (Petrov & Kovalev 2025). The

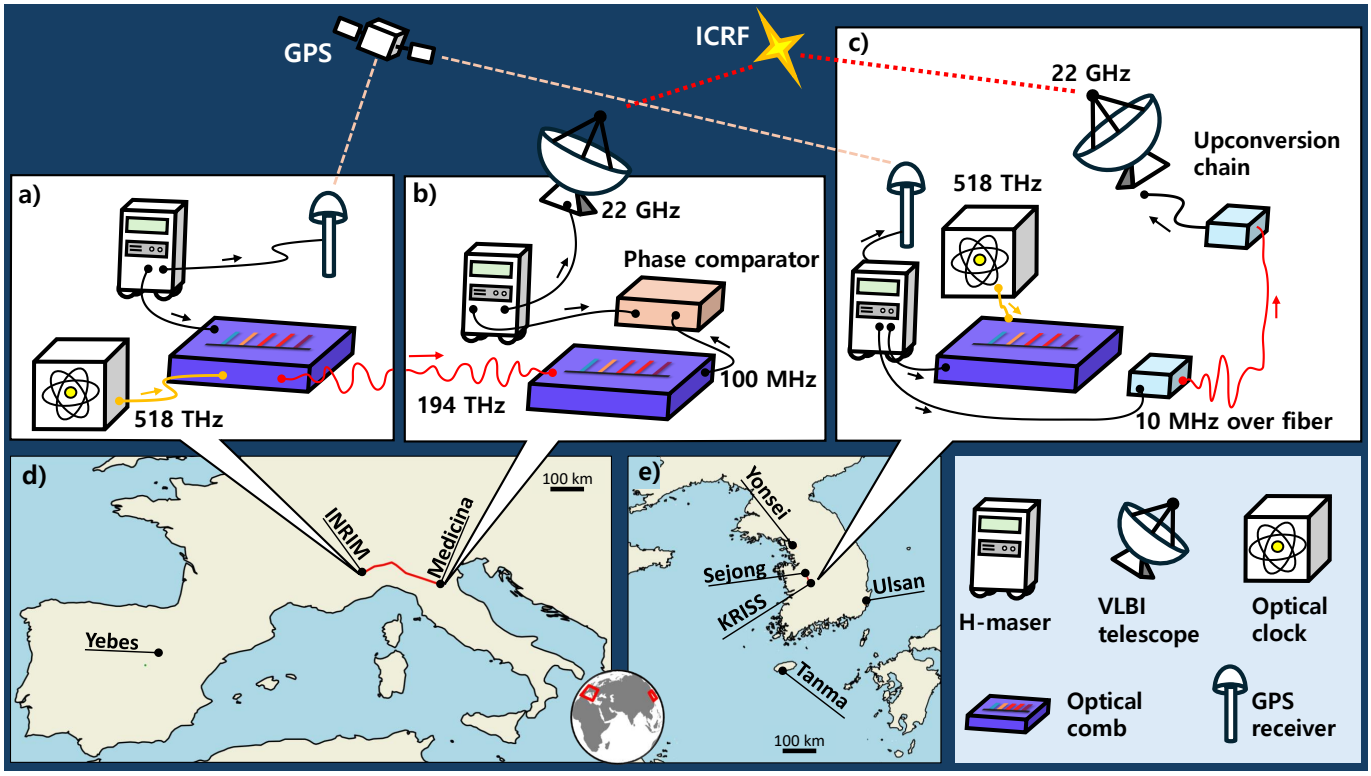

Figure 1. Schematic view of the full experiment setup. (a) At INRIM, in Italy, radiation from an infrared laser is referenced to IT-Yb1 clock via an optical comb and sent to Medicina with a phase-stabilized fiber. IT-Yb1 was also compared to KRISS-Yb1 via a GPS link, using INRIM H-maser as flywheel oscillator. (b) In Medicina, the incoming radiation is coherently converted to a radiofrequency and used to calibrate the local H-maser, which is used for the VLBI observation. (c) In Korea, a 10 MHz signal referenced to a H-maser is sent to Sejong VLBI antenna with a phase-stabilized fiber; here, after demodulation, it seeds the antenna synthesis chain and is used for VLBI observation. KRISS H-maser is also calibrated by KRISS-Yb1 and compared to INRIM via GPS. (d) and (e) Map of Europe and Korea with involved telescopes and Metrological Institutions.

best 69 targets, ranked primarily by sky coverage, were automatically selected by *SKED* for the six-station network during the observation. The sequence of source scans is well-separated in hour angle and elevation over time to improve astrometric accuracy and help separate the tropospheric effect from other parameters. A total of 451 scans were scheduled, each with an integration time of 120 s per source. We recorded right circular polarization (RCP) at a frequency range between 21,184 and 21,696 MHz with a total data rate of 2048 Mbps. The total bandwidth of 512 MHz was divided into 16 intermediate frequency (IF) bands.

2.4. Optical Clocks and Fiber Distribution

To calibrate H-masers, we used KRISS-Yb1 and IT-Yb1, two Yb optical lattice clocks both with systematic uncertainty of 2×10^{-17}, (Kim et al. 2021; Goti et al. 2023). Both clocks contribute regularly to the generation of the International Atomic Time (TAI). INRIM and KRISS are also equipped with GNSS receivers for time transfer. The main reference oscillator at KRISS is a H-maser (KRISS-HM) traceable to UTC (KRIS); its frequency is calibrated by KRISS-Yb1 via an optical frequency comb. The 10 MHz signal from the hydrogen maser is transferred to the Sejong VLBI antenna via a 50 km fiber link. We used a commercial fiber optic frequency distribution system (OSTT, PikTime) to actively compensate for fiber noise (Figure 1(c)).

The additive noise resulting from the fiber link was measured in KRISS to be 10^{-13} at 1 s and 2×10^{-16} at 10^4 s, so the fiber link did not degrade the performance of the VLBI measurement.

In Italy, the Medicina telescope is connected to INRIM via a 535 km optical fiber which is part of the IQB. Among other research facilities, this infrastructure connects two of the main Italian radio telescopes, Medicina and Matera, and has already been used to carry out a common-clock VLBI experiment (Clivati et al. 2020). The frequency distribution chain is based on an ultrastable laser, stabilized at INRIM to a high-finesse Fabry–Perot cavity and calibrated by IT-Yb1 via an optical comb (Figure 1(a)). The optical signal is sent to Medicina and here used to reference a second optical comb, from which an ultra-low noise microwave at 10 GHz and 100 MHz is extracted and phase compared to the local H-maser (Medicina-HM) (Figure 1(b)). The fiber is stabilized using the

Doppler noise stabilization technique, so that the frequency signal delivered at the telescope has a stability of a few parts in 10^{-14} at 1 s and $<10^{-16}$ at 10^4 s (Clivati et al. 2015).

3. VLBI Observation and Data Analysis

3.1. Observation Overview

The 24 hr VLBI experiment was carried out at 6 stations from UTC 2021 December 16 19:00 to 2021 December 17 19:00. The weather conditions were different between Europe and the Republic of Korea. The weather was good in Medicina and Yebes while snow and strong wind were reported at the Sejong station. The KVN observations were completed without any major problems. Approximately, the last seven hours of Yebes data at the end of the experiment were not recorded, thus affecting the last part of the experiment.

The optical clock and fiber-based distribution systems operated almost continuously from a few hours before to a few hours after the campaign. During the 24 hr-long campaign IT-Yb1 and KRISS-Yb1 had an uptime of 94% and 97% respectively. The GNSS link was operational during the campaign without interruption.

3.2. VLBI Data Correlation and Fringe Fitting

Data was transferred from each station to the Daejeon and Bologna Correlators and here processed to compute pairwise interference fringes (fringe-fitting) and extract relative delays between pairs of antennas ($\tau_{\mathrm{obs,\ i,j}}$). In detail, we used the Distributed FX (DiFX) correlation software (Deller et al. 2007), by performing fast Fourier transform (FFT) followed by a complex multiplication of the raw visibilities data of each antenna taken in pairs. Prior to this, the estimation of parameters such as station positions and velocities, source coordinates, and Earth orientation parameters were calculated to achieve the best possible delay model using the Calc software (Gordon et al. 2017).

After the correlation was completed, the DiFX files were converted into Mark4 directories and then fringe-fitted using Haystack Observatory Postprocessing System *fourfit* (Hoak et al. 2022). In the fringe fitting procedure the peak intensity as a function of delay and delay rate is computed scan by scan and sub-band by sub-band and then applied to the fringe visibility data in order to flatten the phases in the frequency channels in each sub-band. Manual phase calibration and Lower Side Band (LSB) offset were inserted for all stations before running the fitting routine.

After the fringe fitting was applied, the data appeared in the Mark3 format, but the commonly used software programs for geodetic data analysis work with databases. For this reason the Mark3 fringe fitting output files were converted into vgosDb (Bolotin et al. 2017) databases containing observed delays, a priori models, instrumental delays corrections and weather parameters.

3.3. Geodetic Data Analysis

Pairwise delays derived as described in Section 3.2 were then fitted with a global model to extract quantities reported in Equation (1). The data analysis software νSolve (Bolotin et al. 2014) was used to analyze the vgosDb database, named 21DEC16XF. νSolve solves for the normal equation calculating the adjustments of a set of parameters by comparing model group delays with observed ones on antenna pairs for each source scan in an observing session. The software estimates the clock parameters through a quadratic model (offset, clock rate, and quadratic term, which corresponds to the relative frequency drift) plus a piece-wise linear function. All these clock parameters are estimated with respect to a reference clock, in this work the Medicina H-maser. Tropospheric parameters, station positions and EOPs are also estimated in the single session solution.

For verification of any possible systematic errors in the analysis, an additional analysis was conducted using the Vienna VLBI & Satellite Software for astrometry and geodesy (VieVS) (Böhm et al. 2018), developed by the Vienna Geoinformatics Group. Unlike νSolve, which performs ionospheric correction only in dual-band sessions (e.g., S/X-band), VieVS is able to perform ionospheric delay correction even in single-band sessions (e.g., K-band). It utilizes GNSS-generated Global Ionospheric Maps (GIMs) to compute ionospheric correction at the position of each station at the time of each observing scan in the session. Such maps have a latitude/longitude resolution of $2.^{\circ}5/5.^{\circ}0$ and are provided daily by the International GNSS Service (IGS) through the Crustal Dynamics Data Information System (CDDIS) repository (Noll 2010). The corrections obtained from this external model were applied to the observing session database.

4. Results

4.1. Comparison via VLBI

νSolve was run on the 21DEC16XF database using standard settings for the parametrization, in order to estimate the clock model parameters (CL0: offset; CL1: clock rate and CL2: quadratic term) needed for clock comparison. As stated in Section 3 no ionospheric corrections were applied as the data set is single-band. After the least-square minimization using 5793 observation pairs, a weighted rms (WRMS) of the group delay residuals of 25.55 ps was obtained, which is the difference between the observed time delay (measured by the radio telescopes) and the theoretical delay (calculated based on known models) and quantifies the overall quality of the experiment. The group delay residuals as a function of observing time are shown in Figure 2 (top). The estimates of

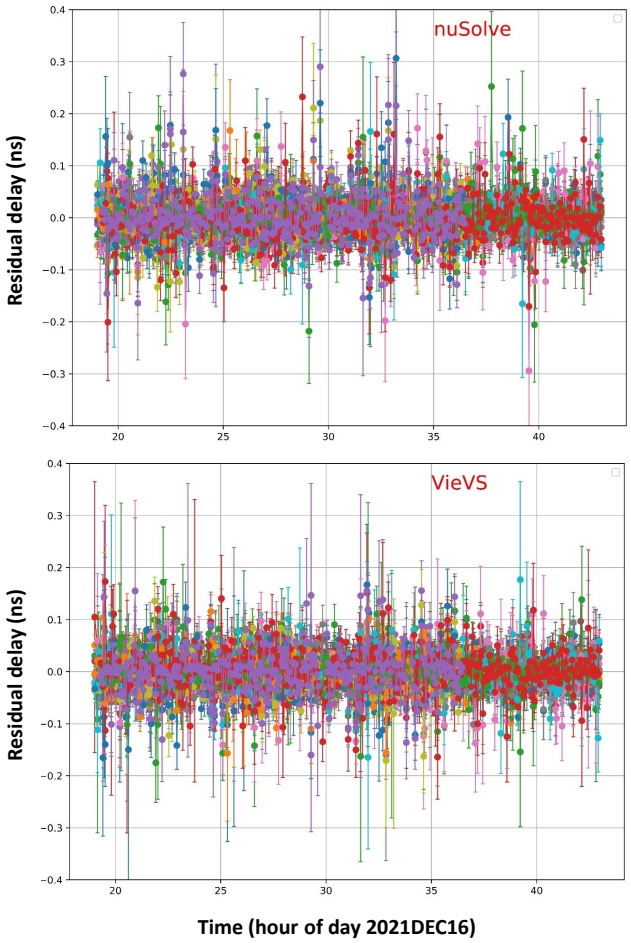

Figure 2. Group delay residuals as a function of observing time during the 2021 December geodetic session obtained by νSolve (top) and by VieVS (bottom). Different colors represent the results of distinct baselines.

the second term CL1 and third term CL2 of the clock model are reported in Table 1.

VieVS was run on the same database using standard settings for the parametrization. The main differences with νSolve concerned the use of the VMF3 mapping function (Landskron & Bohm 2018) for the troposphere parameters estimation, and of the a priori GPT3 model (Landskron & Bohm 2018) for estimating their azimuthal gradients. Two VieVS solutions were obtained with and without the application of the ionospheric correction, respectively. There was no significant difference between the two solutions. The bottom plot in Figure 2 shows the group delay residuals with the ionospheric correction applied. Using 5784 observation pairs, we obtained a WRMS of 26.41 ps. The estimates of the clock rate CL1 and quadratic term CL2 of the clock model are reported in Table 1. Specifically, we assumed CL1 as evaluated with VieVS to be the fractional frequency difference y between the HMs in Medicina and KRISS obtained by VLBI, y(KRISS-HM - Medicina-HM, VLBI) $= -212.5(1.1) \times 10^{-15}$.

Table 1
Relative Difference in Frequency CL1 and its Drift CL2 of the H-maser at Sejong from that at Medicina Obtained from the Geodetic Analysis Performed on νSolve and VieVS

Tool	CL1 (1×10^{-15}) s s^{-1}	CL2 (1×10^{-15}) day^{-1}
νSolve	−214.3 (1.5)	2.1 (2.3)
VieVS	−212.5 (1.1)	−0.7 (1.0)

We adopted clock parameters obtained using VieVS as the best estimation because they were obtained using a better tropospheric and ionospheric modeling. However, the two methods were consistent within uncertainty.

4.2. Comparison by Optical Clocks

H-masers used for the VLBI measurements at Sejong and Medicina were calibrated by KRISS-Yb1 and IT-Yb1. By calibration we mean that the absolute frequencies of the two masers are derived from the comparison with optical clocks, as the two Yb clocks are secondary representations of the SI second (Margolis et al. 2024). In calculating the frequency difference between two H-masers we will assume that, being based on the same atomic species, the two Yb clocks have the same frequency within their uncertainty. In this way, we calculated the average relative frequency difference y of the masers during the campaign, determined by optical clocks (OC), as y(KRISS-HM—Medicina-HM, OC) $= -213.29(14) \times 10^{-15}$. Here the uncertainty includes the instability (7×10^{-18} and 1.1×10^{-17}) and the systematic uncertainty of the clocks (2×10^{-17} and 2×10^{-17}) respectively for IT-Yb1 and KRISS-Yb1. The uncertainty includes an extrapolation uncertainty of 4×10^{-17} for Medicina-HM and 7×10^{-17} for KRISS-HM due to the dead-time in the optical clock measurements calculated from the known noise of the two masers (Yu et al. 2007; Hachisu & Ido 2015). This approach is common for optical clocks operating intermittently (Grebing et al. 2016; Leute et al. 2016; Hachisu et al. 2017; Pizzocaro et al. 2020, 2021; Nemitz et al. 2021). The frequency conversion of the combs introduces an uncertainty of 5×10^{-17} in Medicina and 11×10^{-17} in Sejong. The optical fiber link connecting IT-Yb1 in Torino to the H-maser in Medicina has been characterized to better than 1×10^{-18} and contributes negligibly to the uncertainty of the measurement.

We note that in 2021 December the optical clocks IT-Yb1 and KRISS-Yb1 provided an extended set of data to contribute to the realization of TAI. IT-Yb1 contributed 5 days of data (MJD 59564-59569) that appeared in Circular T n. 410. KRISS-Yb1 contributed 35 days of data (MJD 59544-59579) that appeared in Circular T n. 408. A direct comparison of the two measurements shows the agreement of the two optical

clocks with the relative frequency difference of y(IT-Yb1—KRISS-Yb1) = 3(12) × 10^{-16}, where the uncertainty (1.2×10^{-15}) was limited by satellite link over the 5 days measurement time of IT-Yb1 as appeared in Circular T, and where we included an extrapolation uncertainty using the TAI stability to consider the different measurement time of the two clocks (Pizzocaro et al. 2021). Still, consistency in the two clocks at the 10^{-17} level is expected from the two uncertainty budgets.

4.3. Comparison via GNSS

A GPS-based independent and calibrated time and frequency transfer link was established to validate the VLBI intercontinental link, using two geodetic receivers for timing applications at INRIM and KRISS. These receivers track the code and phase signals emitted by the GPS satellites, and allow comparing them with the internal receiver clock, in turns synchronized and frequency locked to the external signal that is object of comparison. At INRIM, two Septentrio PolaRx4-TR receivers were used, connected to UTC (IT) and the H-maser at INRIM; at KRISS, a GTR55 receiver (MESIT asd) was used to connect to KRISS H-maser which is the master clock for KRISS-Yb1. Among various possible processing algorithms, we chose the PPP (Héroux & Kouba 2001) as it includes the compensation of a significant set of atmosphere, geodynamics, and satellite effects (Héroux & Kouba 2001). Intending PPP as a way of processing, different implementations are available worldwide. We chose NRCan PPP, produced by Natural Resources Canada and optimized for timing applications also with contribution of INRIM, now in use for more than 10 yr by the BIPM for the computation of the TAI and UTC international timescales. Precise IGS estimations for GPS satellites' orbits and clocks were retrieved from the IGS repositories.

The PPP solution was obtained by processing data for the period including the VLBI campaign from MJD 59562 to MJD 59571 and by combining them with data from the optical-VLBI link.

We calculate the average difference of the maser frequency during the campaign using GPS as y(KRISS-HM—Medicina-HM, GPS) = $-215.7(2.0) \times 10^{-15}$.

The uncertainty is limited by the averaging time of the PPP solution over 1 day. We note that other campaigns using GPS data at INRIM (Clivati et al. 2022) revealed a possible problem with the GPS solution at the level of 3×10^{-16} in the considered period of time. This effect is negligible for the measurement presented here.

5. Discussion

5.1. VLBI-GPS-Optical Clock Comparison

The three measurements of the average maser frequency difference obtained with VLBI, optical clocks and GPS are presented in Table 2. From these values we can calculate three closure differences as shown in Table 3. These measurements show good agreement between the different techniques. In particular the agreement between the VLBI measurement and the optical clock measurement is within 2σ, confirming VLBI's potential as a competitive intercontinental clock comparison method. We also note that the estimated frequency drift (CL2) from VLBI analysis via VieVS ($0.7(1.0) \times 10^{-15}$ day^{-1}) is comparable within uncertainty with the drift obtained from optical clocks ($0.7(2.7) \times 10^{-16}$ day^{-1}).

Table 2
Average Frequency Difference in Relative Units of the H-masers at Sejong and Medicina During the Campaign, Measured Using VLBI, the GPS Link and the Calibration by Optical Clocks

	Maser Frequency Difference y (1×10^{-15})	Uncertainty u_{tot} (1×10^{-15})
VLBI	−212.5	1.1
GPS	−215.7	2.0
Optical clocks	−213.29	0.14

Table 3
Closure Difference in the Relative Units of the Measurements Obtained from the Three Techniques

	Closure Difference $\Delta y(1 \times 10^{-15})$	Uncertainty $u_{tot}(1 \times 10^{-15})$
VLBI—OC	0.8	1.1
GPS—OC	−2.4	2.0
VLBI—GPS	3.2	2.3

Given the uncertainties achieved in this first campaign, the results are presented in terms of H-maser frequency differences. Within this framework, optical clock data are used to evaluate the VLBI link. However, these results can also be interpreted as a demonstration of VLBI-based optical clock comparison, which may serve as a valuable complement to existing intercontinental methods.

The results in Table 2 confirm previous findings (Pizzocaro et al. 2021) that VLBI has the potential to achieve lower uncertainties than GPS over similar durations. However, it is important to note that GPS, especially with advanced iPPP algorithms (Petit 2021), can achieve uncertainties in the low 10^{-16} range over several days. Therefore, assessing whether standard VLBI systems can reach this level of accuracy is crucial. For evaluating this capability, continuous week-long VLBI sessions, such as geodetic campaigns, are preferable to multiple shorter campaigns. This approach, however, introduces significant challenges, including increased data volume, complex pre-processing, and more demanding analysis compared to GPS-based clock comparisons.

5.2. High-frequency Geodetic VLBI Observation

This pilot study aimed to assess whether high-frequency VLBI observations can reliably determine clock parameters. Our *K*-band experiment, which employed a total bandwidth of 512 MHz composed of 16 consecutive frequency channels of 32 MHz each, achieved group delay residuals of approximately 26 ps for both νSolve and VieVS, indicating promising performance. Further improvements are anticipated through the use of broader bandwidths and higher observing frequencies.

To enhance group delay precision, we plan to deploy Compact Triple-band Receivers (CTRs; Han et al. 2017), capable of operating across the $K/Q/W$ bands (18–115 GHz), thereby enabling broadband VLBI. With full frequency coverage, the expected group delay uncertainty is projected to reach the sub-picosecond level (∼0.2 ps), as previously demonstrated by the KVN system, which operated over a frequency range of 19.584 to 92.576 GHz using 16 channels of 512 MHz each (total data rate of 32 Gbps).

Additionally, recent results from KVN (Xu et al. 2024) have shown that geodetic VLBI observations at frequency up to 132 GHz are feasible, validating the approach for high-precision astrometry and geodesy. A follow-up campaign is scheduled for 2026, following the upgrade of the Medicina radio telescope with a CTR, to evaluate whether such enhancement can deliver anticipated improvements in group delay accuracy.

5.3. Atmospheric Effects: Troposphere and Ionosphere

Accurate modeling of tropospheric delays is essential for reliable estimation of clock parameters. The VieVS software provided improved parameterization by employing the VMF3 mapping function and GPT3 a priori model (Landskron & Bohm 2018). In addition, the KVN-style simultaneous multi-frequency system has proven highly effective in calibrating tropospheric phase fluctuations in the millimeter-wave regime through the use of the Frequency Phase Transfer (FPT) method (Jung et al. 2011; Rioja et al. 2015; Rioja & Dodson 2020), in which high-frequency observations are calibrated using scaled solutions from lower-frequency data. We expect that applying FPT in conjunction with CTRs and enhanced tropospheric modeling will enable effective VLBI observations at high frequencies, despite challenges such as atmospheric opacity and turbulence. This has already been demonstrated in a recent study using the KVN (Xu et al. 2024).

Ionospheric corrections applied using Global Ionospheric Maps (GIMs) in VieVS showed negligible influence on the estimated clock parameter in this experiment. This finding is consistent with results from Xu et al. (2024), who tested both GNSS-based Global Ionospheric Maps and dual-frequency VLBI combinations. Although ionospheric effects are minimal over the relatively short KVN baselines, they can become significant on longer intercontinental baselines due to global variations in Total Electronic Content (TEC), potentially introducing delays of several tens of picoseconds. Nonetheless, the KVN-style simultaneous multi-frequency receivers (e.g., CTRs) are expected to mitigate ionospheric impact across the 18–115 GHz range. This is because (1) the ionosphere imposes a frequency-dependent phase shift that diminishes at higher frequencies, and (2) simultaneous observations at multiple bands allow comparing and compensating dispersive delays, thereby improving phase calibration and group-delay precision —even for longer intercontinental baselines such as Korea–Italy.

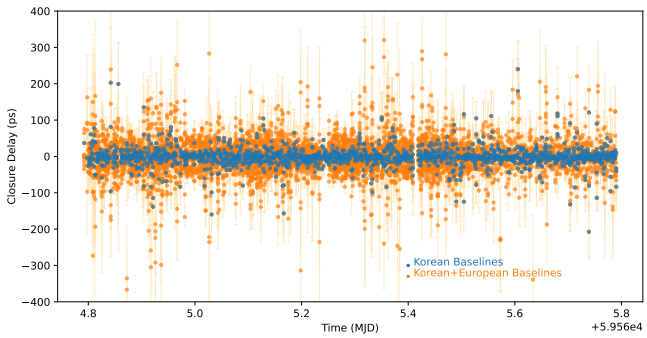

Figure 3. Closure delays during the experiment. Blue and orange dots represent closure delays for Korean baselines (KVN and Sejong) and Korean–European baselines, respectively.

A more comprehensive assessment of atmospheric effects on clock parameter estimation using high-frequency, wideband VLBI observations is planned for 2026, coinciding with the anticipated deployment of upgraded CTR systems.

5.4. Source Structure Effects and Instrumental Delays

The *K*-band sources used in this study were selected from the ICRF3 and AstroGeo databases. Source structure remains a major contributor to uncertainty in geodetic VLBI, particularly at lower frequencies, where non-closure delays may arise and impact baseline solutions (Bolotin et al. 2019; Xu et al. 2019; Pizzocaro et al. 2021; Sekido et al. 2021). Observations at higher frequencies, as enabled by CTRs, are expected to alleviate these issues due to the more compact nature of radio sources (e.g., Charlot et al. 2010; de Witt et al. 2023).

Figure 3 presents the closure delay results from our analysis, showing a WRMS of 20.1 ps across all baselines and a significantly lower value of 5.8 ps for Korean-only baselines. This discrepancy may result from: (1) source structures being resolved over longer (∼9000 km) baselines, (2) lower SNRs for fringe detection on those baselines, (3) the absence of instrumental phase calibration (PCAL) systems, or a combination of these and other residual errors.

At the KVN and Sejong stations, round-trip monitoring systems are deployed to ensure stable distribution of reference frequency from the observatory building to the receiver cabin.

More recently, advancements in the KVN-style multi-frequency system have introduced the integration of optical frequency comb (OFC)-based technologies. These systems generate and distribute phase-coherent, low-noise RF signals that are locked to atomic (or, optical in near future) clock references. This enables precise calibration of instrumental phase offsets and frequency-dependent variations across multiple receiver bands (Hyun et al. 2026). Photonic PCAL systems of this kind are particularly important for ultra-broadband (multi-frequency) VLBI astrometry and geodesy, including optical clock comparison experiments.

Future improvements in source structure delay modeling and the deployment of CTRs with integrated PCAL are expected to yield multiple benefits. First, incorporating more telescopes on intermediate baselines would enable more robust source imaging, aiding in the estimation and calibration of source structure effects. Second, improved instrumental calibration would allow for quantitative separation of delay contributions due to source structure versus instrumentation. This would support the identification of optimal VLBI targets (i.e., point-like sources) and enable precise evaluation of source structure effects, particularly for intercontinental baselines.

6. Conclusion and Future Prospect

As a pilot study for optical clock comparison using existing VLBI networks, we designed, organized, and implemented a geodetic VLBI campaign at *K*-band. This experiment serves as a precursor to the deployment of new high-frequency broadband receivers (e.g., CTR), which will soon be installed at several VLBI stations. This new infrastructure is expected to be utilized by many scientific research efforts, and we specifically aim to explore its application in metrology. Therefore, our pilot campaign was conducted as a standard geodetic observation, utilizing *K*-band, standard scheduling, and analysis techniques, with the primary goal of identifying the potential and critical points of this methodology. The results obtained in this work with different approaches were in agreement at the 10^{-15} s s^{-1} level, which states that standard geodetic VLBI campaigns could be used for intercontinental clock comparisons, currently only possible via satellite techniques.

In the future, an optimal frequency setup in the range 18–115 GHz will be studied to optimize the next VLBI observations. This will exploit the new high-frequency broadband receivers (CTRs), which have demonstrated their effectiveness in improving the accuracy of the resulting group delays (Xu et al. 2024). As a result, they will allow a better estimation of the clock parameters of the stations.

We plan to carry out longer experiments with a larger network including other international stations equipped with the same receivers, which will allow us to connect to the international metrology community. This will bring with it additional challenges because of the large amount of data that will have to be stored and transferred via the network to the correlators in Italy and Korea. Nevertheless, this network has the potential to provide the metrology community with a high-performing and independent method for intercontinental clocks comparisons.

Acknowledgments

This research was supported by the National Research Council of Science and Technology (NST) grant by the Korea government (MSIT) (No. CAP22061-000) and Measurement Technology for Grand National Strategic industries funded by KRISS (KRISS-2026-GP2026-0012). The observations and correlations are supported through the high-speed network connections among the KVN and Sejong stations provided by the KREONET (Korea Research Environment Open NETwork), which is operated by the KISTI (Korea Institute of Science and Technology Information). Roberto Ricci acknowledges the support of the European Research Council through the Consolidator grant BHianca (Grant agreement ID: 101002761). The authors thank the anonymous referee who helped improve the presentation of this work to a wider audience.

Facilities: Medicina:32m, Sejong, KVN, Yebes:40m.

Software: SKED (Gipson 2010), *DiFX* (Deller et al. 2007), *fourfit* (Hoak et al. 2022), νSolve (Bolotin et al. 2014), *VieVS* (Böhm et al. 2018).

ORCID iDs

Monia Negusini https://orcid.org/0000-0002-0064-5533
Myoung-Sun Heo https://orcid.org/0000-0002-9231-3789
Cecilia Clivati https://orcid.org/0000-0002-7289-6403
Shuangjing Xu https://orcid.org/0000-0003-2953-6442
Roberto Ricci https://orcid.org/0000-0003-4631-1528
Taehyun Jung https://orcid.org/0000-0001-7003-8643
Buseung Cho https://orcid.org/0000-0002-4661-5700
Matteo Stagni https://orcid.org/0000-0003-0294-0365
Claudio Bortolotti https://orcid.org/0000-0002-6480-4564
Giuseppe Maccaferri https://orcid.org/0000-0002-1482-708X
Federico Perini https://orcid.org/0000-0002-8935-8142
Mauro Roma https://orcid.org/0000-0003-4142-3897
Do-Young Byun https://orcid.org/0000-0003-1157-4109
Do-Heung Je https://orcid.org/0009-0003-6409-3218
Marco Pizzocaro https://orcid.org/0000-0003-2353-362X
Davide Calonico https://orcid.org/0000-0002-0345-859X
Elena Cantoni https://orcid.org/0000-0002-2332-2534
Giancarlo Cerretto https://orcid.org/0000-0002-4486-7138
Stefano Condio https://orcid.org/0000-0003-4921-7959
Giovanni A. Costanzo https://orcid.org/0000-0002-7474-0349
Simone Donadello https://orcid.org/0000-0002-9565-1214
Irene Goti https://orcid.org/0000-0002-4826-6495

Michele Gozzelino https://orcid.org/0000-0001-8783-5665
Alberto Mura https://orcid.org/0000-0001-8922-4729
Filippo Levi https://orcid.org/0000-0002-0206-9082
Matias Risaro https://orcid.org/0000-0001-8046-5710
Huidong Kim https://orcid.org/0000-0002-1623-5520
Won-Kyu Lee https://orcid.org/0000-0002-2142-8343
Chang Yong Park https://orcid.org/0000-0002-3139-6728
Dai-Hyuk Yu https://orcid.org/0000-0001-7796-7664
Young Kyu Lee https://orcid.org/0000-0003-2753-5227
Joon Hyo Rhee https://orcid.org/0000-0001-7304-3624
Chanjin Park https://orcid.org/0009-0002-7557-9881
Minseong Lee https://orcid.org/0000-0002-1774-2831
Hyo Ryoung Kim https://orcid.org/0009-0004-4853-1019
Sung-Moon Yoo https://orcid.org/0000-0001-6280-8222
Jungho Cho https://orcid.org/0000-0002-3482-1232
Jongsoo Kim https://orcid.org/0000-0002-1229-0426
Ha Su Yoon https://orcid.org/0000-0001-9917-5246
Pablo de Vicente https://orcid.org/0000-0002-5902-5005

References

Akatsuka, T., Goh, T., Imai, H., et al. 2020, OExpr, 28, 9186
Bauch, A., Achkar, J., Bize, S., et al. 2005, Metro, 43, 109
Beloy, K., Bodine, M. I., Bothwell, T., et al. 2021, Natur, 591, 564
Böhm, J., Böhm, S., Boisits, J., et al. 2018, PASP, 130, 044503
Bolotin, S., Baver, K., Bolotina, O., et al. 2019, in Proc. 24th Meeting of the European VLBI Group for Geodesy and Astrometry, https://www.ign.es/resources/acercaDe/libDigPub/Proceedings_EVGA_2019_v2_digital.pdf
Bolotin, S., Baver, K., Gipson, J., Gordon, D., & MacMillan, D. 2014, in IVS 2014 General Meeting Proc. VGOS: The New VLBI Network, https://ivscc.gsfc.nasa.gov/publications/gm2014/054_Bolotin_etal.pdf
Bolotin, S., Baver, K., Gipson, J., Gordon, D., & MacMillan, D. 2017, in European VLBI Group for Geodesy and Astrometry Working Meeting 23, ed. R. Haas & G. Elgered, 235
Boven, E. P., Koelemeij, J. C. J., van Tour, C., et al. 2026, ExA, 61, 3
Brewer, S. M., Chen, J.-S., Hankin, A. M., et al. 2019, PhRvL, 123, 033201
Charlot, P., Boboltz, D., Fey, A., et al. 2010, AJ, 139, 1713
Charlot, P., Jacobs, C. S., Gordon, D., et al. 2020, A&A, 644, A159
Chiodo, N., Quintin, N., Stefani, F., et al. 2015, OExpr, 23, 33927
Clark, D. L., Cage, M. E., Lewis, D. A., & Greenlees, G. W. 1979, PhRvA, 20, 239
Clivati, C., Aiello, R., Bianco, G., et al. 2020, Optic, 7, 1031
Clivati, C., Costanzo, G. A., Frittelli, M., et al. 2015, ITUFF, 62, 1907
Clivati, C., Pizzocaro, M., Bertacco, E., et al. 2022, PhRvP, 18, 054009
Counselman, C., Shapiro, I., Rogers, A., et al. 1977, IEEEP, 65, 1622
Deller, A. T., Tingay, S. J., Bailes, M., & West, C. 2007, PASP, 119, 318
de Witt, A., Jacobs, C. S., Gordon, D., et al. 2023, AJ, 165, 139
Dierikx, E. F., Wallin, A. E., Fordell, T., et al. 2016, ITUFF, 63, 945
Dimarcq, N., Gertsvolf, M., Mileti, G., et al. 2024, Metro, 61, 012001
Droste, S., Ozimek, F., Udem, T., et al. 2013, PhRvL, 111, 110801
Fujieda, M., Piester, D., Gotoh, T., et al. 2014, Metro, 51, 253
Gill, P. 2016, JPhCS, 723, 012053
Gipson, J. 2010, in IVS 2010 General Meeting Proc. No. NASA/CP 2010-215864, 77, https://ivscc.gsfc.nasa.gov/publications/gm2010/gipson2.pdf
Gordon, D., Ma, C., MacMillan, D., et al. 2017, International VLBI Service for Geodesy and Astrometry 2015+2016 Biennial Report, TP–2017–219021, NASA 224, http://ivscc.gsfc.nasa.gov/publications/br_2015_2016/acgsfc.pdf
Goti, I., Condio, S., Clivati, C., et al. 2023, Metro, 60, 035002
Grebing, C., Al-Masoudi, A., Dörscher, S., et al. 2016, Optic, 3, 563
Grotti, J., Koller, S., Vogt, S., et al. 2018, NatPh, 14, 437
Hachisu, H., Fujieda, M., Nagano, S., et al. 2014, OptL, 39, 4072
Hachisu, H., & Ido, T. 2015, JaJAP, 54, 112401
Hachisu, H., Petit, G., Nakagawa, F., Hanado, Y., & Ido, T. 2017, OExpr, 25, 8511
Han, S.-T., Lee, J.-W., Lee, B., et al. 2017, JIMTW, 38, 1487
Hoak, D., Barrett, J., Crew, G., & Pfeiffer, V. 2022, Galax, 10, 119
Hurd, W. J., Wardrip, S. C., Bussion, J., et al. 1979, The Deep Space Network Progress Report 42-49, Jet Propulsion Laboratory, https://ipnpr.jpl.nasa.gov/progress_report/42-49/49J.PDF
Husmann, D., Bernier, L.-G., Bertrand, M., et al. 2021, OExpr, 29, 24592
Hyun, M., Ahn, C., Choi, J., et al. 2026, Light Sci Appl, 15, 53
Héroux, P., & Kouba, J. 2001, PCEA, 26, 573
Jung, T., Sohn, B. W., Kobayashi, H., et al. 2011, PASJ, 63, 375
Kim, H., Heo, M.-S., Park, C. Y., Yu, D.-H., & Lee, W.-K. 2021, Metro, 58, 055007
Krehlik, P., Buczek, Ł., Kołodziej, J., et al. 2017, A&A, 603, A48
Krishnan, V. V., Bailes, M., van Straten, W., et al. 2020, Sci, 367, 577
Landskron, D., & Bohm, J. 2018, JGeod, 92, 349
Lange, R., Huntemann, N., Rahm, J. M., et al. 2021, PhRvL, 126, 011102
Ledbetter, M., Kowligy, A., Roslund, J., et al. 2025, in International Technical Meeting 2025, https://www.ion.org/itm/abstracts.cfm?paperID=15127
Leute, J., Huntemann, N., Lipphardt, B., et al. 2016, ITUFF, 63, 981
Lisdat, C., Grosche, G., Quintin, N., et al. 2016, NatCo, 7, 12443
Lodewyck, J. 2019, Metro, 56, 055009
Margolis, H. S., Panfilo, G., Petit, G., et al. 2024, Metro, 61, 035005
McGrew, W. F., Zhang, X., Fasano, R. J., et al. 2018, Natur, 564, 87
Musha, M., Hong, F.-L., Nakagawa, K., & Ueda, K.-i. 2008, OExpr, 16, 16459
Nakamura, T., Davila-Rodriguez, J., Leopardi, H., et al. 2020, Sci, 368, 889
Nemitz, N., Gotoh, T., Nakagawa, F., et al. 2021, Metro, 58, 025006
Noll, C. E. 2010, AdSpR, 45, 1421
Oh, H., Kondo, T., Lee, J., et al. 2010, in IVS 2010 General Meeting Proc. No. NASA/CP 2010-215864, 449, https://ivscc.gsfc.nasa.gov/publications/gm2010/ohsejin.pdf
Petit, G. 2021, GPSS, 25, 22
Petrov, L. Y, & Kovalev, Y. Y 2025, ApJS, 276, 38
Pizzocaro, M., Bregolin, F., Barbieri, P., et al. 2020, Metro, 57, 035007
Pizzocaro, M., Sekido, M., Takefuji, K., et al. 2021, NatPh, 17, 223
Raymond, A. W., Doeleman, S. S., Asada, K., et al. 2024, AJ, 168, 130
Rieck, C., Haas, R., Jarlemark, P., & Jaldehag, K. 2012, in 2012 European Frequency and Time Forum, 163
Riedel, F., Al-Masoudi, A., Benkler, E., et al. 2020, Metro, 57, 045005
Riehle, F., Gill, P., Arias, F., & Robertsson, L. 2018, Metro, 55, 188
Rioja, M. J, & Dodson, R. 2020, A&ARv, 28, 6
Rioja, M. J., Dodson, R., Jung, T., & Sohn, B. W. 2015, AJ, 150, 202
Sanner, C., Huntemann, N., Lange, R., et al. 2019, Natur, 567, 204
Schuh, H., & Behrend, D. 2012, JGeo, 61, 68
Sekido, M., Takefuji, K., Ujihara, H., et al. 2021, JGeod, 95, 41
Serrano, J., Alvarez, P., Cattin, M., et al. 2009, in Int. Conf. Accelerator and Large Experimental Physics Control Systems (ICALEPCS), 2009, https://proceedings.jacow.org/icalepcs2009/papers/tuc004.pdf
Takamoto, M., Ushijima, I., Ohmae, N., et al. 2020, NaPho, 14, 411
Ushijima, I., Takamoto, M., Das, M., Ohkubo, T., & Katori, H. 2015, NaPho, 9, 185
Xie, X., Bouchand, R., Nicolodi, D., et al. 2017, Opt. Lett., 42, 1217
Xu, M. H., Anderson, J. M., Heinkelmann, R., et al. 2019, ApJS, 242, 5
Xu, M. H., & Charlot, P. 2025, AJ, 169, 173
Xu, S., Jung, T., Zhang, B., et al. 2024, AJ, 168, 219
Yu, D.-H., Weiss, M., & Parker, T. E. 2007, Metro, 44, 91